3002–3015 *Nucleic Acids Research, 2007, Vol. 35, No. 9* *Published online 16 April 2007*
doi:10.1093/nar/gkm196

CAF1 plays an important role in mRNA deadenylation separate from its contact to CCR4

Takbum Ohn, Yueh-Chin Chiang, Darren J. Lee, Gang Yao, Chongxu Zhang and Clyde L. Denis*

Department of Biochemistry and Molecular Biology, University of New Hampshire, Rudman Hall, Durham, NH 03824, USA

Received December 6, 2006; Revised March 19, 2007; Accepted March 20, 2007

ABSTRACT

The CAF1 protein is a component of the CCR4–NOT deadenylase complex. While yeast CAF1 displays deadenylase activity, this activity is not required for its deadenylation function *in vivo*, and CCR4 is the primary deadenylase in the complex. In order to identify CAF1-specific functional regions required for deadenylation *in vivo*, we targeted for mutagenesis six regions of CAF1 that are specifically conserved among CAF1 orthologs. Defects in residues 213–215, found to be a site required for binding CCR4, reduced the rate of deadenylation to a lesser extent and resulted in *in vivo* phenotypes that were less severe than did defects in other regions of CAF1 that displayed greater contact to CCR4. These results imply that CAF1, while affecting deadenylation through its contact to CCR4, has functions in deadenylation separate from its contact to CCR4. Synthetic lethalities of *caf1Δ*, but not that of *ccr4Δ*, with defects in DHH1 or PAB1, both of which are involved in translation, further supports a role of CAF1 separate from that of CCR4. Importantly, other mutations in PAB1 that reduced translation, while not affecting deadenylation by themselves or when combined with *ccr4Δ*, severely blocked deadenylation when coupled with a *caf1* deletion. These results indicate that both CAF1 and factors involved in translation are required for deadenylation.

INTRODUCTION

In eukaryotes, the major pathway of mRNA degradation is initiated by poly(A) tail shortening (deadenylation) followed by removal of the 5′ cap structure (decapping) and 5′–3′ exonucleolytic cleavage of the mRNA body by the XRN1 exonuclease (1–3). Deadenylation, as compared to decapping and 5′–3′ nuclease digestion, has been shown to be most important in the control of mRNA degradation rates (4). The CCR4-NOT complex in responsible for the majority of the poly(A) shortening process in yeast (5–7), and its 1.0 MDa core complex is comprised of 10 components: CCR4, CAF1 (also known as POP2), five NOT proteins (NOT1–NOT5), CAF40, CAF130 and BTT1 (8–11). Of these proteins, CCR4 and CAF1 appear to be the most important players in the mRNA deadenylation process (5,6).

The CCR4 protein as a member of ExoIII family of nucleases/phosphatases (12,13) is the catalytic subunit responsible for degradation of the mRNA poly(A) tail, and point mutations in the predicted active site of CCR4 cause deadenylation defects like that of a *ccr4* deletion (5,7). Similarly, a *ccr4* mutant in *Drosophila* also displayed an *in vivo* deadenylation defect, as did reduction in CAF1 levels (14).

The role of the CAF1 protein, however, is less clear. Its principal role has been considered to be that of linking CCR4 to the remainder of the CCR4-NOT complex (8,9,15,16). Deletion of the *CAF1* gene showed a dramatic deadenylation defect *in vivo*, albeit to a lesser extent than that of *ccr4Δ* (6), and this has been interpreted to mean that CCR4 must be part of the CCR4-NOT complex to function well *in vivo*. Although CAF1 is classified as a member of the DEDDh family of nucleases (17,18) and the polypeptide isolated from *Escherichia coli* can function as a 3′–5′ exonuclease with some preference for poly(A) sequences (19,20), inactivation of predicted key catalytic active sites of CAF1 did not affect *in vivo* deadenylation function (16). Moreover, overexpression of *CCR4* could partially complement the deadenylation defect of a *caf1* deletion, but overexpression of *CAF1* did not rescue phenotypes associated with that of a *ccr4* deletion (6,7). These results indicate that the deadenylase activity of CAF1 is not required for its *in vivo* deadenylation function. Moreover, CAF1 has been shown recently to interact with PUF5 and to be

*To whom correspondence should be addressed. Tel: +1-603-862-2427; Fax: +1-603-862-4013; Email: cldenis@cisunix.unh.edu

required for PUF5-induced deadenylation of mRNA (21), supporting other roles of CAF1 in mRNA deadenylation.

Since the predicted catalytic sites of CAF1 are not critical to its *in vivo* function, understanding the functional roles of CAF1 on mRNA turnover will require the identification of other important regions of the CAF1 protein. To identify in the CAF1 protein functional regions, which are critical for mRNA degradation, we conducted a deletion analysis of yeast CAF1 by targeting regions absolutely conserved among CAF1 orthologs. This mutation analysis identified four functional regions of CAF1, including those required for binding CCR4 and for deadenylation. Domains of CAF1 that are important to deadenylation *in vivo* included but are not limited to those that are required for CCR4 binding. Relatedly, defects in CAF1, but not that in CCR4, were lethal with defects in DHH1 (33) and PAB1, factors involved in translation, and over-expression of translation-associated proteins could suppress *caf1Δ pab1* lethality. Moreover, we showed that a PAB1 translation defect severely reduced deadenylation when coupled with a *caf1* deletion. CAF1, in addition to binding CCR4, may act on the deadenylation process in conjunction with factors affecting translation.

MATERIALS AND METHODS

Yeast strains and growth conditions

The background yeast strains used in this study are listed in Table 1. Yeast strains were grown in YEP medium (2% yeast extract, 1% Bacto peptone) or minimal medium supplemented with nutrients required for auxotrophic deficiencies and with 4% glucose or 2% galactose/2% raffinose unless otherwise indicated. YD plates consisted of YEP medium supplemented with 2% glucose and 2% agar and caffeine plates are YD plates with 5, 8 or 15 mM caffeine as indicated.

Library screening for high-copy suppressors and analysis of synthetic lethalities

Strain ASY319-c1-lN/YC360/YC506 was transformed with a YEp13 (2 μ *LEU2*) high-copy yeast genomic library and plated on minimal medium lacking leucine and tryptophan. Here, ~15 000 Leu^+ transformants were plated onto plates containing 5-fluoroorotic acid (FOA). The plasmids from yeast capable of growth on FOA plates were rescued, transformed into *E. coli*, rescued and retransformed into the original strain to confirm the high-copy suppression. Yeast genomic sequences within the plasmids were identified by DNA sequence analysis. In cases where more than two yeast genes were located on the plasmid insert, such as for *DHH1* and *CAF1*, the MPT1 and MPT0 plasmids carrying only *DHH1* and *CAF1*, respectively, were used to confirm that these genes were responsible for the suppression of the lethality (29). *caf1Δ* lethality with *PAB1-ΔRRM2* or with *PAB1-ΔRRM1* was determined by transforming strain AS319-c1-lN/YC360 with YC504, YC505 and YC506, respectively. Following selection of these YC504/YC505/YC506 transformants, their ability to survive in the presence of the *caf1Δ* allele was determined by the transformants' abilities to lose the YC360 (*URA3*) plasmid and grow on FOA-containing plates. Testing for the lethality of deletions in other genes and *PAB1-ΔRRM2* was done by a similar methodology.

Site-directed deletion mutagenesis

The MPT0 plasmid harboring the yeast *CAF1* open reading frame was used as the template for the polymerase chain reaction (PCR). All PCR reactions were performed with Vent polymerase (New England Biolabs). In order to generate 173DVW175, 213FRS215, 255WQF257, 303SGL305, 329LMN331 and 340DFE342 deletions, we designed the following six pairs of oligonucleotide primers: caf1-1-f (5′-TATCTTTTCGTTCGCAAGTCC AACCTTTACAGTGAATTC-3′) and caf1-1-r (5′-GTAAAGGTTGGACTTGCGAACGAAAAGATAATT TGGGG-3′), caf1-2-f (5′-AGGCCGATCGGCA CTAAGGTCGATTACCACTATCAGACA-3′) and

Table 1. List of yeast strains

Strain	Genotype
EGY188	*MATa ura3 his3 trp1 LexA–LEU2*
EGY188-c1	Isogenic to EGY188 except *caf1* :: *URA3*
EGY188-c1-1	Isogenic to EGY188 except *caf1* :: *ura3*
EGY188-1a-1-c1	Isogenic to EGY188 except *ccr4* :: *ura3 caf1* :: *LEU2*
EGY191	*MATα ura3 his3 trp1 LexA–LEU2*
EGY191-c1	Isogenic to EGY191 except *caf1* :: *URA3*
KY803-c1	*MATa leu2-PET56 trp1-Δ1 ura3-52 gal2 gcn4-Δ1 caf1 :: LEU2*
AS319/YC504	*MATα ura3 leu2 his3 trp1 pab1 :: HIS3* [PAB1-TRP1]
AS319-1a-uN/YC504	Isogenic to AS319 except *ccr4* :: *ura3* :: *NEO*
AS319-c1-lN/YC504	Isogenic to AS319 except *caf1* :: *leu2* :: *NEO*
AS319-cl-lN/YC505/YC360	Isogenic to AS319-cl-lN except [PAB1-ΔRRM1-TRP1] [PAB1-URA3]
AS319-cl-lN/YC506/YC360	Isogenic to AS319-cl-lN except [PAB1-ΔRRM2-TRP1] [PAB1-URA3]
AS319-d1-uL/YC504	Isogenic to AS319 except *dhh1* :: *ura3* :: *LEU2*
1743-2/YC504	*MATα ura3 leu2 his3 trp1 pab1 :: HIS3 [PAB1-TRP1] prt1-63*
1881/YC504	Isogenic to AS319 *except cdc33-1*
A1385-uT-c1/TB3	*MATa ura3 leu2 his3 trp1 dhh1 :: ura3 :: TRP1 caf1 :: LEU2* [GAL1-CAF1-URA3]

caf1-2-r (5′-GTGGTAATCGACCTTAGTGCCGATCG GCCTAGCCAAAGT-3′), caf1-3-f (5′-AACGGTCC CTCAACGAATTTTGAATTTGACCCAAAGAAG-3′) and caf1-3-r (5′-GTCAAATTCAAAATTCGTTGAGGG ACCGTTGTCAGGCTT-3′), caf1-4-f (5′-CAGCTTCT AATGGACATGATGGATGATTCTGTTACTTGG-3′) and caf1-4-r (5′-AGAATCATCCATCATGTCCATTAG AAGCTGCGAAAATTC-3′), caf1-5-f (5′-TTCCTGAT CAACATTGACTCCATGCCCAACAACAAGGAG-3′) and caf1-5-r (5′-GTTGGGCATGGAGTCAATGTT GATCAGGAAACCTAGATC-3′), and caf1-6-f (5′-CCCAACAACAAGGAGTGGTGGGTCCATCAATA CATGCCC-3′) and caf1-6-r (5′-TTGATGGAC CCACCACTCCTTGTTGTTGGGCATGGAGTC-3′). These primers were used for the first PCR reaction in combination with primers containing BamHI and HindIII restriction sites Caf1-Bm-f (5′-AAAGGATCCATGC AATCTATGAATGTACAA) and caf1/2291-Hind (5′-TACATATAAAGCTTAAATGATCATTGGTCCC-3′). The first PCR products were used for amplifying final full-length *CAF1* mutant alleles using Caf1-Bm-f and caf1/2291-Hind primers. The final PCR products were purified, digested with BamHI and HindIII, and inserted into BamHI- and HindIII-digested pET-23a(+) to generate plasmids pTB8a (*CAF1*), pTB8-1 (*caf1-1*), pTB8-2 (*caf1-2*), pTB8-3 (*caf1-3*), pTB8-4 (*caf1-4*), pTB8-5 (*caf1-5*) and pTB8-6 (*caf1-6*), respectively. All the sequences of the mutagenized *CAF1* alleles were verified by sequencing. For further analysis, *CAF1* open reading frames were subcloned into pLexA202-2 (22), pJG4-5 (22) and pJCN112 (7) to make N-terminal LexA, HA and N-terminal Flag with C-terminal 6His epitope tagged CAF1 proteins, respectively. pLexA202-2 fusions were constructed to allow constitutive high expression of *CAF1* from an *ADH1* promoter, and the other two fusions were to allow galactose-inducible expression of *CAF1* from a *GAL1* promoter. LexA-CAF1 fusions were also used in certain cases because they were carried on a *HIS3*-containing plasmid that allowed it to be co-transformed with *URA3*-based plasmids, such as those carrying Flag-CAF1, Flag-CCR4 and Flag-PAB1.

Flag pull-down analysis

The yeast cultures containing Flag-CAF1 fusions were grown to late log phase in 50 ml selective medium supplemented with 4% glucose, shifted to 100 ml of the same medium with 2% galactose/raffinose and grown for 16 h. The cells were washed and lysed by the glass bead method in extraction buffer (50 mM Tris–Cl [pH7.9], 150 mM NaCl, 0.1 mM $MgCl_2$, 0.1% NP40, 20% glycerol) plus a protease inhibitor cocktail. After clarification of the crude cell lysates by centrifugation at 15 000 × *g* at 4°C for 15 min twice, the supernatants were incubated with 400 µl of anti-Flag M2 affinity agarose (Sigma) at 4°C overnight. The bound resins were washed with 10 ml wash buffer (extraction buffer with 5% glycerol) three times, transferred to microfuge tubes and washed with 1 ml wash buffer five times. The resultant precipitates were run subsequently on an 8% SDS-polyacrylamide gel, electro-transferred to polyvinylidene fluoride (PVDF) membrane (Immobilon™-P, Millipore) and analyzed by western blot using SuperSignal® West Pico Luminol/ Enhancer Solution (Pierce).

Protein extraction, *in vitro* deadenylation assays and *in vivo* translation assays

Flag-CCR4 protein purification was performed as described above for purification of Flag-CAF1 with some modifications (23). The strain EGY188-c1-1a-1 harboring single copy of CCR4 (pYC343) and the LexA-CAF1 fusion variants were grown in 1 l of selective medium with 4% glucose to mid-log phase (OD_{600} of 0.7). Following lysis and incubation of supernatants with the anti-Flag M2 antibody-agarose (Sigma), the Flag agarose beads were washed with 10 ml of washing buffer three times, and the Flag fusion proteins were eluted twice with extraction buffer containing 200 µg/ml Flag peptide (Sigma). *In vitro* deadenylation assays were conducted as described (16,23). The rates of *in vivo* protein synthesis were determined by quantitating the amount of [^{35}S]-methionine incorporation into protein as described (24).

RNA preparation and analyses

RNA samples were prepared using the hot acidic phenol method described in Ref. (25). Briefly, yeast cells were resuspended in TES (10 mM Tris–Cl [pH 7.5], 10 mM EDTA, 0.5% SDS) and the acidic phenol and incubated at 65°C for 45 min with frequent vortexing. Following centrifugation, the supernatants were re-extracted with acidic phenol and chloroform. RNA present in the supernatants was precipitated with 95% ethanol and dissolved in water containing DEPC.

To perform the transcriptional pulse-chase experiments, strain EGY188-cl carrying the individual LexA-caf1 variants was grown in 5 ml of synthetic medium supplemented with 2% raffinose, transferred and regrown in 100 ml fresh medium until mid-log phase (OD_{600} of 0.7). Cells were then harvested, washed once with fresh medium and transferred to 15 ml of fresh medium containing 2% raffinose and grown for 15 min. *GAL1* transcription was activated by adding galactose at a 2% final concentration for 15 min and shut-off by adding glucose to a concentration of 4%. Since yeast cells harboring the LexA–caf1-2 protein resulted in poor *GAL1* transcription, the *GAL1* promoter was activated for 30 min prior to transcription shut-off.

The deadenylation rates and end points for *GAL1* mRNA were determined following RNase H treatment of purified RNAs as described previously (26). Here, ~4 µg of an oligonucleotide probe (5′-GCCATTTGGGCCC CCTGG-3) complementary to a segment 133 bp upstream of the *GAL1* translational stop codon was hybridized with 12 µg of total RNA prior to RNase H digestion. The resultant *GAL1* 3′ polyadenylated species were separated on a denaturing polyacrylamide gel (6%/7.5 M urea) and detected by northern analysis using a probe complementary to the 3′ end of the *GAL1* mRNA (5′-GCCCAATGCTGGTTTAGAGACGATGATAGCA TTTTCTAGCTCAGCATCAGTGATCTTAGGG-3). The rate of deadenylation was determined for the shortest

poly(A) tail as previously described (6,16). Calculating the rate of deadenylation using the average length of poly(A) gave similar results.

For steady-state *MFA2pG* mRNA analyses, strains were grown to exponential phase (OD_{600} of 0.4) in selective medium supplemented with 2% raffinose. Cells were then transferred to fresh medium for an hour, and the *GAL1* promoter was induced for 3 h following the addition of galactose.

RESULTS

Mutagenesis of CAF1 in the regions that are highly conserved among CAF1 orthologs

In order to identify CAF1-specific functional regions, we targeted for mutagenesis the regions of CAF1 that are common only to CAF1 orthologs and are not present in any other DEDDh nuclease family members (17,18). Six regions were identified as absolutely conserved among CAF1 orthologs (Figure 1B). Three amino acid deletions were made in each case to remove the region of homology, resulting in *caf1* alleles 1 through 6. After these deletions were constructed and their phenotypes obtained, the X-ray crystallographic analysis of the C-terminal RNase D domain of CAF1 protein was published (19). The relative locations of each of the constructed *caf1* alleles are shown in Figure 1A: *caf1-1* (173DVW175) and *caf1-3* (255WQF257) alleles are positioned in β-sheets β1 and β4 that hydrogen bond to each other, *caf1-2* (213FRS215) is located between β2 and α3 in a crystallographically undefined loop region, and *caf1-4* (303SGL305), *caf1-5* (329LMN331) and *caf1-6* (340DFE342), are located in a turn at the end of α6, just at the beginning of a turn after α7, and on α8, respectively.

Each of the *caf1* mutant alleles was subsequently cloned into three types of plasmid vectors, pLexA(202), pJG4-5 (HA-tagged) and pJCN112 (Flag-tagged), for further analysis (see Materials and Methods section). Each of the mutant proteins, regardless of the epitope attached to CAF1, was expressed to comparable levels as that found for the wild-type CAF1 protein, indicating that these small deletions did not affect the protein expression or stability of CAF1 (Figures 2A,B and 4A).

Phenotypic analysis of *caf1* alleles

One of the most prominent phenotypes of a strain carrying a *caf1* deletion is its caffeine sensitivity, although other phenotypes such as temperature sensitivity and slow growth have been observed (15,28,29). To examine the phenotypes of *CAF1* mutant alleles, we tested the growth phenotypes of the *caf1* alleles by using the KY803-c1 (*caf1Δ*) strain carrying a plasmid expressing an N-terminal Flag fusion with each of the mutant CAF1 proteins (Figure 3; summarized in Table 2). Of the six *CAF1* mutants, *caf1-1*, *caf1-3* and *caf1-6* alleles resulted in an inability to grow on YD plates containing 5 mM caffeine. Interestingly, strains carrying the *caf1-1* and *caf1-3* alleles were observed to grow slower on rich medium lacking caffeine than a strain carrying the *caf1* null allele (data not shown). The *caf1-2* and *caf1-5* alleles caused weak sensitivity to caffeine, and for the *caf1-4* allele, we did not observe any difference in growth on caffeine plates as compared to the wild-type strain. The same results were obtained with LexA-CAF1 fusions (data not shown).

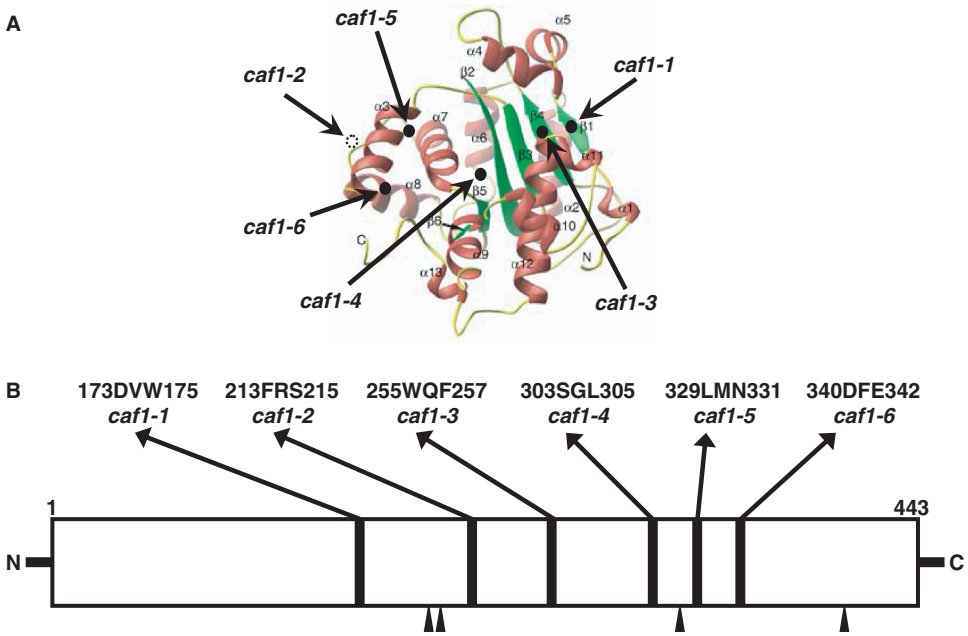

Figure 1. Mutagenesis of CAF1. (**A**) Location of *CAF1* mutations are illustrated on the 3D structure of the nuclease domain of the CAF1 protein (19). (**B**) The six absolutely conserved regions targeted for mutagenesis are composed of three amino acids each as indicated above the schematic representation of CAF1 and are located in regions separate from the putative four key catalytic amino acids conserved among DEDDh ribonucleases (black arrows). The names of the mutant alleles are also shown beneath the deleted amino acids.

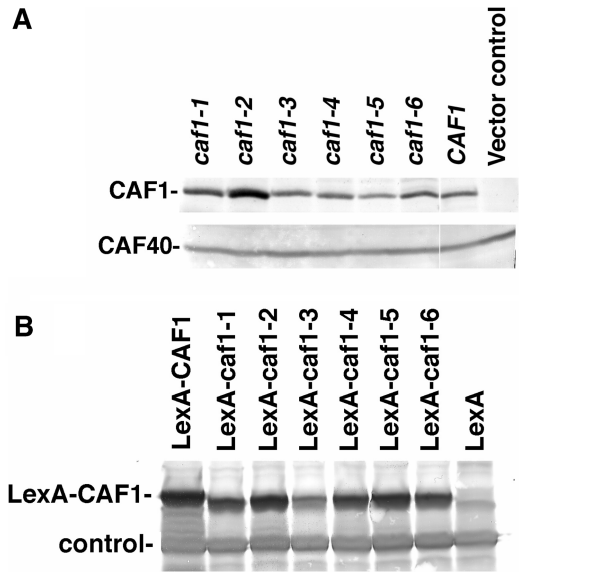

Figure 2. Western blot analysis of CAF1 mutant proteins. (**A**) The HA-CAF1 proteins were expressed in the EGY191-c1 strain, protein extracts were made and the CAF1 proteins were detected by western analysis. The apparent increased abundance of caf1-2 protein in the gel that is presented is artifactual and no significant differences in the abundance of these proteins were observed in numerous other experiments. Vector control refers to pJG4-5 without the CAF1 protein. Equivalent amounts of protein were loaded in each lane as determined by Bradford assay, and western analysis using CAF40 (lower panel), CCR4 and NOT3 antibodies confirmed equivalent levels of CAF40, CCR4 and NOT3 proteins in each of the lanes. (**B**) The LexA-CAF1 proteins were expressed in EGY188-c1 and the CAF1 proteins were detected by western analysis using LexA antibody. The cause for the multiple bands present for CAF1 is not known, but they are not related to the phosphorylation of CAF1 that has previously been observed (27). The control band refers to a non-specific protein that interacts with the LexA antibody and indicates that nearly equivalent amounts of protein were loaded into each lane.

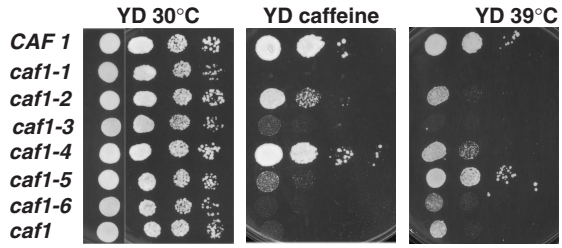

Figure 3. Growth of strains carrying *caf1* alleles. Yeast strains (KY803-c1 with Flag-CAF1 variants as indicated or with pJCN112, no Flag-CAF1, *caf1*) were grown on YD plates at 30°C, on YD plates with 5 mM caffeine, or on YD plates at 39°C. In each panel, moving from left to right 10-fold less cells were plated in each column. Initial concentrations of cells were $\sim 1 \times 10^7$ cells/ml for the left row and 4 µl of sample was placed in each spot.

In terms of temperature-sensitive growth, strains carrying the wild-type and *caf1-5* alleles were able to grow at 39°C (Figure 3; Table 2), whereas those containing the *caf1-1* and *-3* alleles failed to grow at 39°C. The strain with *caf1-4* grew weakly at 39°C, and strains carrying *caf1-2* and *-6* grew very weakly. In order to verify that the deletion of three consecutive amino acid residues

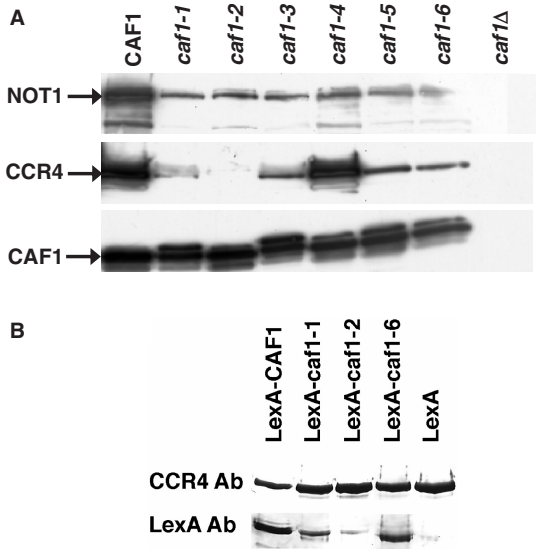

Figure 4. *caf1-2* is deficient in contacting CCR4 *in vivo*. (**A**) N-terminal FLAG tagged *CAF1* alleles were transformed into the *caf1* deletion strain, KY803-c1. Crude extracts (5 mg) were immunoprecipitated with anti-FLAG M2 antibody and proteins were visualized by western blot analysis with antibodies directed against CCR4, NOT1 and CAF1 as indicated. (**B**) Plasmids expressing LexA-CAF1 were transformed into strain EGY188-1a-1-c1 containing Flag-CCR4 expressed from its own promoter on a centromere-containing plasmid. Flag-CCR4 was purified as described for Flag-CAF1, and LexA antibody was used to identify CAF1 as indicated.

Table 2. Growth phenotypes of yeast cells carrying *caf1* mutant alleles

CAF1 allele	5 mM caffeine	39°C
Wild-type	+	+
caf1-1	−	−
caf1-2	w	w/−
caf1-3	−	−
caf1-4	+	w
caf1-5	w/−	+
caf1-6	−	w/−
caf1Δ	−	w/−
caf1-10	w	w/−
caf1-11	−	−

KY803-c1 strains carrying FLAG-CAF1 proteins or pJCN112 vector alone (*caf1Δ*) were tested. Growth was detected on YEP plates containing 2% glucose (YD) and supplemented with 5 mM caffeine. Temperature sensitive growth was monitored on YD plates at 39°C. +, good growth; w, weak growth; −, no growth

did not dramatically affect the structure of the protein and result in the caffeine- and temperature-sensitive phenotypes that were observed, we constructed two additional *caf1* alleles in which three alanine residues were substituted for the three residues deleted in *caf1-2* and *caf1-3*. These two alleles were chosen in that results shown below indicated that the *caf1-1* and *caf1-6* alleles appeared phenotypically similar to *caf1-3*, and *caf1-2* was unique for being most defective in CCR4 binding. Strains carrying *caf1-10* (213AAA215) and *caf1-11* (255AAA257) displayed the exact same phenotypes as did strains with their respective deletion alleles, *caf1-2* and *caf1-3* (Table 2). For the remainder of our analysis the original

deletion mutations were used. It should also be noted that these *CAF1* deletion derivatives, as has been previously observed for *caf1* deletions (8–10), did not affect the relative protein amounts and, therefore, expression in the cell of other CCR4-NOT components, such as CCR4, NOT1, NOT3 or CAF40 (data not shown).

The caf1-2 protein is defective in binding with CCR4

The relative locations of the proteins in the CCR4-NOT core complex have been determined (9–11) in which the CAF1 protein is critical for linking CCR4 to NOT1 and the remainder of the CCR4-NOT complex. We, therefore, assessed the ability of each of the CAF1 mutant proteins to bind CCR4 and NOT1, using Flag-tagged CAF1 protein variants expressed in a *caf1* deletion background. Flag-CAF1 was used for this analysis as the Flag immunoprecipitations resulted in substantially cleaner backgrounds than immunoprecipitations with either HA- or LexA-CAF1 variants. After Flag immunoprecipitations were conducted, as shown in Figure 4A, we found that the caf1-4 protein was able to bind CCR4 as well as wild-type CAF1. The caf1-2 protein, in contrast, was totally defective in binding to CCR4 (Figure 4A). The slight band observed in the *caf1-2* lane with CCR4 antibody does not migrate where CCR4 is located and is a result of a non-specific protein interaction. The caf1-1, -3, -5 and -6 proteins also displayed reduced binding to CCR4, but they still displayed significantly more association with CCR4 than did caf1-2. While all of the mutant proteins were still capable of binding NOT1, they did display reduced binding to NOT1 as compared to wild-type CAF1.

In order to verify these results, we also conducted the immunoprecipitation in the reverse direction for several of the key CAF1 variants. Using a Flag-tagged CCR4 and LexA-fused versions of the CAF1 variants, we isolated Flag-CCR4 and determined the abundance of LexA-CAF1 that was co-immunoprecipitated. As shown in Figure 4B, LexA-caf1-2 was most severely deficient in binding CCR4. In contrast, LexA-caf1-1 and LexA-caf1-6 proteins bound significantly better to CCR4 than did LexA-caf1-2. However, as demonstrated in Figure 4A, both the LexA-caf1-1 and LexA-caf1-6 proteins were still defective in binding CCR4 as compared to wild-type CAF1 (Figure 4B).

These above results suggest several conclusions. First, the immunoprecipitation data indicate that the differences in the growth and caffeine phenotypes described above do not result solely from differences in CAF1 binding NOT1 or CCR4. The severe phenotypes displayed with the *caf1-1*, *-3* and *-6* alleles were not due solely to loss of CCR4 binding, as each of these corresponding proteins could bind CCR4 as well as caf1-5, whose allele did not display as severe growth defects. The caf1-2 protein was most defective for binding CCR4, and yet the strain carrying *caf1-2* grew better than did those carrying *caf1-1*, *-3* or *-6*, indicating that loss of CCR4 binding alone was not the cause for the *caf1* deletion phenotypes. Therefore, while CAF1 binding to CCR4 contributes to part of the defects observed with *caf1Δ*, as exemplified by *caf1-2*, other CAF1 interactions must also be important to its function. Third, the ratio of NOT1-CCR4 in the caf1-1, -3, -5 and -6 immunoprecipitations was similar to that found in the wild-type strain, arguing that some of the CCR4-NOT complex was intact in the cell. The expression and abundance of the individual CCR4-NOT proteins in the cell were not affected by the caf1 variants as determined by western analysis (data not shown), suggesting that the each of the caf1 variants except for caf1-4 was causing some destabilization of the CCR4-NOT complex. Yet, as the strain carrying *caf1-5* was similar to wild type in terms of its growth at high temperature, the reduced abundance of the CCR4-NOT complex *per se* is not the sole cause for all of the severe growth defects observed with *caf1-1*, *-3* and *-6*. These observations also suggest that the severe growth defects of *caf1-1*, *-3* and *-6* relative to that of *caf1-2* and *caf1-5* are not specifically due to the caf1-1, -3 and -6 proteins being completely misfolded and hence comparable to the *caf1Δ* allele, as some of these caf1-1, -3 and -6 proteins are still capable of binding CCR4 and NOT1.

We also assayed the purified CCR4-NOT complex from each of the mutated strains for *in vitro* CCR4 deadenylation activity (23). CAF1 is not required for CCR4 *in vitro* deadenylation function (7,30), and, as expected, the six *caf1* alleles did not significantly alter CCR4-NOT *in vitro* deadenylation activity following purification of Flag-CCR4 (Supplementary Figure 1). We were not able to assay, however, for CAF1 deadenylase activity *in vitro* since we have not been able to demonstrate enzyme activity for yeast CAF1 (6,16).

Identification of separable functional regions required for mRNA deadenylation

In order to determine if the *caf1* mutant alleles affected mRNA deadenylation *in vivo*, transcriptional pulse-chase experiments were performed on the *GAL1* mRNA. In this experiment, transcription of *GAL1* mRNA was induced by adding galactose and then repressed by adding glucose to the growing culture. Following a 15 min induction, *GAL1* mRNA synthesis was shut-off at time zero and aliquots were prepared for northern analysis at each time point. As shown in Figure 5A, *GAL1* mRNA was shortened with a 3′ oligonucleotide probe and RNase H prior to separation on a denaturing polyacrylamide gel for size resolution of the poly(A) tail. Due to two polyadenylation sites in the *GAL1* gene, *GAL1* mRNAs consists of two forms: *GAL1*-L and *GAL1*-S in which the long *GAL1*-L has an additional 110 nt in its 3′-UTR segment as compared to *GAL1*-S (Figure 5A) (31,32). However, as *GAL1*-S mRNA is less abundant and therefore more difficult to detect and quantitate than that of *GAL1*-L mRNA, we present only the data for *GAL1*-L. Also, for this experiment LexA fusions to the CAF1 variants were used to transform a *caf1* deletion yeast strain so that CAF1 would be constitutively expressed from its *ADH1* promoter.

The deadenylation rate analysis of *GAL1*-L mRNA identified several functional regions in CAF1 that are important for normal deadenylation *in vivo*. Of the six

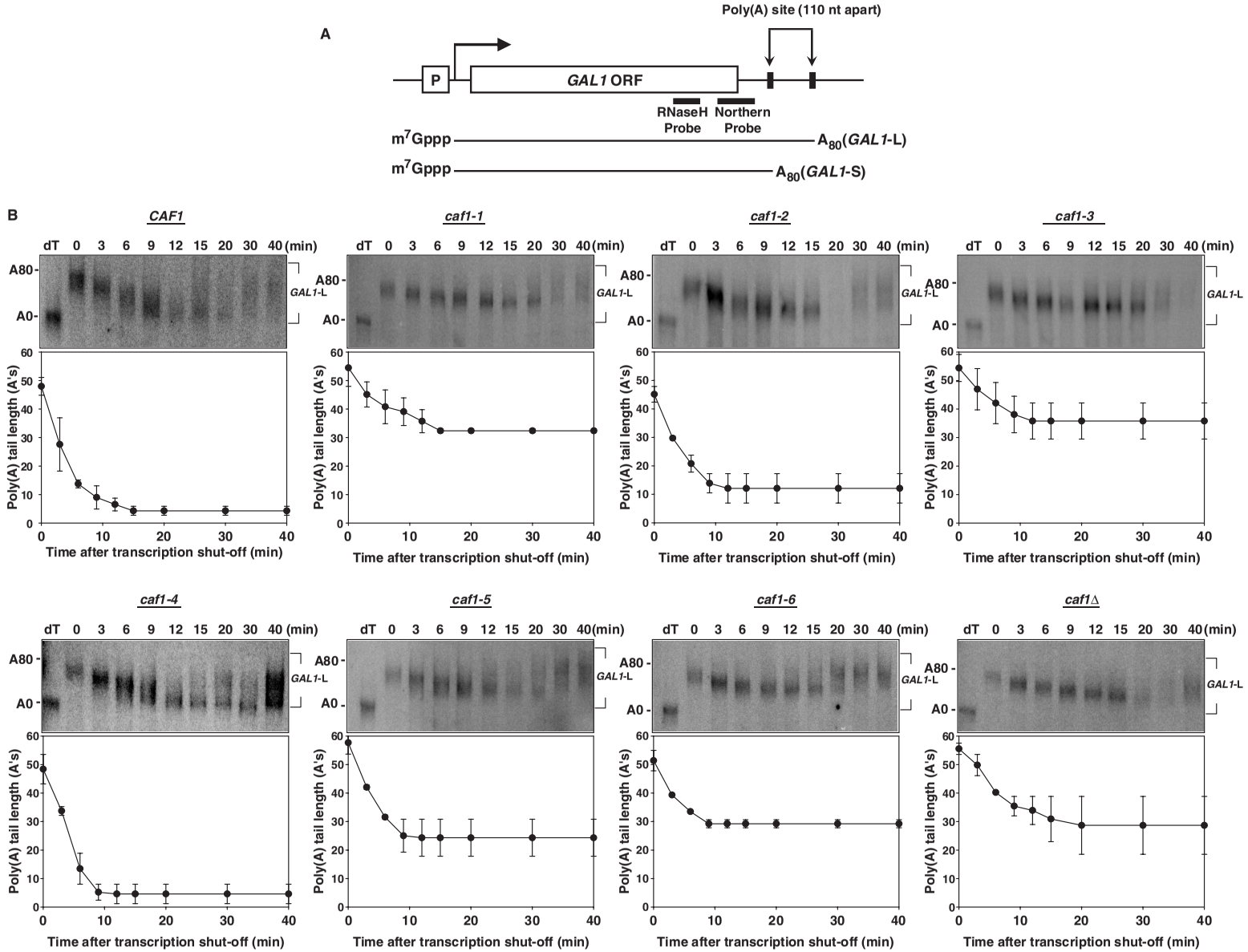

Figure 5. Mutagenesis of CAF1 identifies separable functional regions involved in deadenylation. (**A**) Diagram for the *GAL1* gene and its two mRNAs. (**B**) Transcriptional pulse-chase analyses on *GAL1*-L mRNA were conducted with EGY188-c1 harboring each LexA–*caf1* fusion or the LexA vector as the negative control. Following a 15–30-min induction of the *GAL1* gene by addition of galactose, transcription was shut-off at time zero by adding glucose. Northern blot analyses were conducted with RNA samples prepared from yeast cells harvested at the time points indicated. dT refers to the RNA sample probed with oligo (dT) followed by RNase H digestion to remove the poly(A) tail and represents 0 adenosines (A's). The 80 A's marker size was determined from the known *GAL1*-L and *GAL1*-S deadenylated lengths and from comparing *GAL1*-L poly(A) tail lengths against those of *MFA2pG* in other experiments (16). It should also be noted that at later time points the *GAL1* mRNA synthesis is incompletely turned off by glucose and that at the 30 min time point it is often observed that newly synthesized mRNA with long poly(A) tails become present. This new mRNA does not significantly obscure the data for the original pulse of mRNA synthesis, and their poly(A) tail lengths were not used in the determinations of the poly(A) tail length of the original pulse of mRNA synthesis.

caf1 alleles, *caf1-1*, *caf1-3* and *caf1-6* alleles displayed severe deadenylation rate defects similar to that displayed with a *caf1* null allele. For the wild-type strain (Figure 5B), *GAL1*-L poly(A) tails were shortened to 8–12 nt within 9 min. In contrast, in the *caf1-1*, *-3* and *-6* allele background, *GAL1*-L was only deadenylated to ~30–35 A's within the first 9 min (Figure 5B). Similar defects in *GAL1*-S mRNA deadenylation were also observed for *caf1-1*, *-3* and *-6* as compared to wild type (data not shown). The average rate of deadenylation for *GAL1*-L in wild type was 4.9 A's/min in which the rate of deadenylation was based on the lower end of the poly(A) distribution (26) (Table 3). In the *caf1-1*, *-3* and *-6* mutated strains, the range of the deadenylation rates for *GAL1*-L mRNAs were from 2.0 to 2.9 nt/min (Table 3). For *caf1-2* and *caf1-5*, in contrast, the deadenylation rates for *GAL1*-L were in the 3.4–4.4 A's/min range, indicating that they were defective in deadenylation but not to the extent observed for the *caf1-1*, *-3* and *-6* alleles (Table 3; Figure 5B). *caf1-4* displayed a faster deadenylation rate than wild type. In addition, it should be observed that the caf1-1, -3 and -6 proteins failed to allow complete deadenylation to 8–10 A's even at the 40-min time point. caf1-2 allowed deadenylation to proceed much further to nearly wild-type lengths, whereas caf1-5 displayed a more severe deadenylation endpoint defect with *GAL*1-L. Given that the phenotypic analysis of *caf1-2* and *caf1-5* showed that their temperature and caffeine sensitivities were halfway between wild type and that of the *caf1* deletion, these *in vivo* deadenylation data agree well with their *in vivo* phenotypes.

Table 3. Deadenylation rates of *GAL1* and endpoints of *MFA2pG* mRNA

CAF1 allele	Deadenylation rate (A's/min ± SEM) GAL1-L	Deadenylation endpoint range [oligo(A) shortest to longest ± SEM for longest lengths] MFA2pG
Wild type	4.9 ± 0.5	0–11 ± 1.9
caf1-1	2.0 ± 0.2	5.3–29 ± 3.4
caf1-2	3.4 ± 0.7	1.9–15 ± 2.1
caf1-3	2.1 ± 0.5	5.2–29 ± 3.4
caf1-4	6.1 ± 1.6	0–11 ± 2.1
caf1-5	4.4 ± 0.6	0–12 ± 4.3
caf1-6	2.9 ± 0.7	2.2–24 ± 2.0
*caf1*Δ	2.4 ± 0.5	3.5–26 ± 2.7

caf1 deletion strains (EGY188-c1) harboring LexA versions of wild-type, *caf1* mutants and vector (LexA202-2) were used for transcriptional pulse chase analysis. Rates of deadenylation were measured by the change in the length of the shortest poly(A) tail as a function of time following transcriptional shut-off (Figure 4B). Similar results were obtained using the mean poly(A) tail length. EGY188-c1-1 strains harboring LexA-caf1 variants and pRP485 (*GAL1-MFA2pG*) were used for analyzing steady-state *MFA2pG* mRNA. The range in oligo(A) lengths for the *pG* fragments from northern analysis was taken from deadenylation endpoint measurements. Deadenylation rate values represent the average of three separate experiments and the standard error of the mean (SEM), and the deadenylation endpoints are the average of two separate experiments and the SEM for the longest length poly(A) segments.

To more precisely analyze deadenylation endpoints, the steady-state RNA levels of *MFA2pG* were studied (6). In this case, the *pG* mRNA fragments that results from deadenylation, decapping and 5′ nuclease digestion of *MFA2pG* allows a better estimate of the deadenylation endpoint than does pulse-chase analysis. Previously, a *caf1* deletion has been shown to result in median endpoints of ~16–20 A's as compared to 8–12 A's for wild-type *CAF1* (6). We found that *caf1-1*, *-3* and *-6* alleles resulted in a longer poly(A) tail length for the *pG* fragment that results after deadenylation, decapping and 5′–3′ nuclease action on *MFA2pG* than for wild-type CAF1: 24–29 A's for the longest A lengths as compared to 11 A's for wild-type (Figure 6, lanes 2, 4, 7 compared to lane 1; summarized in Table 3). In the *caf1-2* and *caf1-5* alleles, the deadenylation endpoints of the *pG* fragment were not significantly affected as compared to wild-type (Figure 6, lanes 3, 6; Table 3). It should also be noted that the rate of *MFA2pG* deadenylation appeared slower in the *caf1-1*, *-3* and *-6* backgrounds as compared to *caf1-2*, *-5*, and *CAF1*. In the top part of Figure 6, it can be observed that full-length *MFA2pG* mRNA poly(A) tails are on average significantly longer for *caf1-1, -3,* and *-6* than that of *caf1-2*, *-5* and *CAF1*, indicative of slowed deadenylation. Moreover, the ratio of full-length *MFA2pG* RNA to that of the *pG* fragment was significantly greater for *caf1-1*, *-3* and *-6* as compared to *caf1-2*, *-5*, and *CAF1*, indicating that the rate of decapping and degradation of the *MFA2pG* mRNA was being slowed, most likely due to a slowed rate of deadenylation (6). These overall results indicate that the severe growth phenotypes of *caf1-1*, *-3* and *-6* probably result from the inability of the CCR4-NOT complex to properly deadenylate *in vivo* and that CAF1 must also

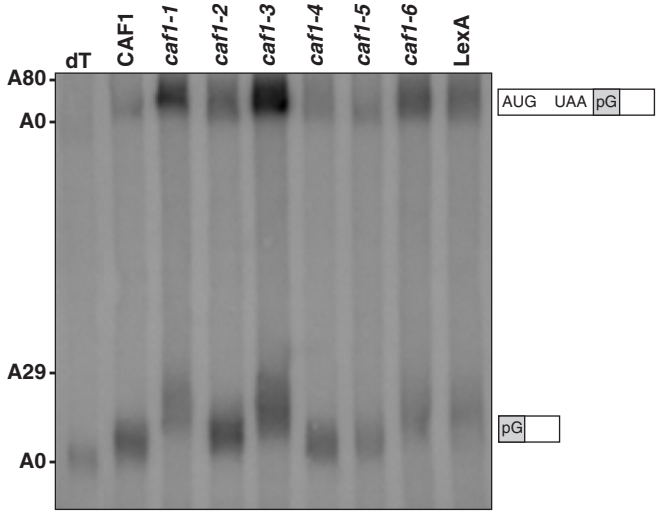

Figure 6. *caf1-1*, *-3* and *-6* alleles are defective in the deadenylation endpoint of the *MFA2pG mRNA*. Northern analysis of steady-state *MFA2pG* mRNA was conducted in a *caf1Δ* background (EGY188-c1-1) in which LexA-CAF1 fusion proteins were expressed as indicated. dT refers to removal of oligo(A) by incubation with oligo(dT) followed by RNase H digestion. The approximate lengths of the poly(A) tail and migration positions of the *MFA2pG* and *pG* fragments are indicated to the left and right, respectively. LexA refers to the LexA vector alone expressed in strain EY188-c1-1.

interfere with the deadenylation process separately from its contacts to CCR4 and NOT1.

Analysis of the role of CAF1 in deadenylation separate from contacting CCR4

The above results support the model that CAF1 has an effect on the mRNA degradation process in addition to that derived from its contact to CCR4. In this regard, the *caf1* deletion has previously been shown to be lethal with a deletion in the decapping/translational regulator *DHH1* whereas the *ccr4* deletion is not lethal with that of *dhh1Δ* (33). In order to determine which *CAF1* allele can confer lethality with *dhh1Δ*, we constructed a strain carrying both a *dhh1Δ* and a *caf1Δ* that was covered by a plasmid expressing a *GAL1-CAF1* gene. This strain was unable to grow on glucose growth conditions when *GAL1-CAF1* expression was shut-off (Supplementary Figure 2). Following transformation of *LexA-CAF1* plasmids encoding each of the above mutagenized *CAF1* alleles, the *caf1-1*, *-3* and *-6* alleles did not allow growth on glucose growth conditions whereas *caf1-2* and *-5* alleles allowed growth on glucose (Supplementary Figure 2). These data suggest that *caf1-1*, *-3* and *-6* alleles are also defective in a non-deadenylation function.

caf1Δ dhh1Δ lethality could result from their combined effects on deadenylation that is separate from CCR4 effects on deadenylation. However, this model is unlikely in that lethality does not occur under circumstances when deadenylation in the cell is completely blocked (6). An alternative model would be that as DHH1 is known to be involved in both decapping (34) and translation (35), CAF1 could be involved separately from CCR4 in either or both of these functions leading to a *caf1Δ dhh1Δ* lethality. This model would further suggest that CAF1 effects on deadenylation that are separate from binding CCR4 would result from its involvement in this other function. That is, CAF1 interaction with the decapping/translation processes may affect deadenylation. However, CAF1 is not probably involved in decapping separately from CCR4. Studies that measured the relative decapping rate using the *MFA2pG* RNA have suggested that the slowed deadenylation observed with a *caf1* deletion does not result in a more severe decapping defect than does *ccr4Δ* (5,6; data not shown).

In an analysis of the genetic interactions of poly(A)-binding protein (PAB1) with CCR4 and CAF1, we observed that deleting the RRM2 or RRM1 domain of PAB1 was lethal with a *caf1* deletion but not with *ccr4Δ*. The RRM2 domain of PAB1 is important both for contacting the poly(A) tail and the translation initiation factor eIF4G, and both RRM1 and RRM2 are required for poly(A) stimulated *in vitro* translation (36–38). This observation suggests that CAF1 has functions separate from CCR4 that involve some role of PAB1. We subsequently analyzed whether deletion of other components of the CCR4-NOT complex or those of the PAN2/3 deadenylase were lethal with these PAB1 variants. We found that the *not4Δ*, *not5Δ* and *caf40Δ*, as well as *pan2Δ* and *pan3Δ*, were not lethal with these PAB1 mutants (data not shown), implying that it was a specific property of CAF1 that resulted in the lethality. This observed *caf1Δ pab1-ΔRRM2* lethality suggests that CAF1 may functionally interact with factors affecting translation, which in turn may affect deadenylation. The RRM1 and RRM2 deletions of PAB1 also reduced the *in vivo* rate of protein synthesis by 28 and 15%, respectively, whereas deletion of RRM3, RRM4 or of the C-terminal region of PAB1 had <6% effects on the rate of protein translation (data not shown). Deletions of RRM3, RRM4 or the C-terminus of PAB1 were correspondingly not lethal with *caf1Δ* (data not shown). We also found that the *caf1-1*, *-3* and *-6* alleles but not those of *caf1-2* or *caf1-5* were lethal with *PAB1-ΔRRM2* (data not shown). These genetic interactions support the possibility that CAF1 is functionally involved with factors that affect the translation process.

To clarify the genetic interaction between *caf1Δ* and *PAB1-ΔRRM2*, we conducted a genetic screen to identify genes whose over-expression could rescue this synthetic lethality. A high-copy YEp13-*LEU2* yeast genomic library was transformed into a strain carrying the *caf1Δ PAB1-ΔRRM2* allele and the YC360 plasmid [PAB1-URA3]. Eleven plasmids that suppressed the *caf1Δ PAB1-ΔRRM2* lethality were identified, as evidenced by their ability to support loss of the YC360 plasmid following growth on 5′-FOA plates. Five of these plasmids contained *CAF1* and one plasmid carried *PAB1*. All of these plasmids suppressed the lethality strongly (Figure 7). Of the remaining five plasmids, two displayed moderate suppression, and of these one was found to carry the *DHH1* gene and the other the *STM1* gene. The remaining three weakly suppressing plasmids will be reported on separately.

Because previous analysis has identified several multi-copy suppressors of a *caf1* deletion, including that of *DHH1*, *CCR4*, *PKC1*, *STM1* and *PUF5* (29), we tested whether over-expression of each of these different genes in a strain carrying *caf1Δ PAB1-ΔRRM2* and *PAB1-URA3* could suppress the *caf1Δ PAB1-ΔRRM2* lethality and allow loss of *PAB1-URA3* and subsequent growth on 5′-FOA media. As shown in Figure 7A, we failed to observe any high-copy suppression of *caf1Δ PAB1-ΔRRM2* by *CCR4*, *PKC1* or *PUF5*. Since over-expression of *CCR4* can complement *caf1Δ* deadenylation defects (6), this last result confirms that *caf1Δ pab1-ΔRRM2* lethality is not due solely to a deadenylation defect. Moreover, it indicates that the ability of over-expressed *DHH1* and *STM1* to complement the *caf1Δ PAB1-ΔRRM2* lethality does not result from simply the ability to complement *caf1Δ* defects. These findings provide additional genetic evidence supporting the functional participation of CAF1 in a process that is separate from the role involving CCR4.

One additional model to explain the role of DHH1 in suppressing the *caf1Δ PAB1-ΔRRM2* lethality would be that over-expression of DHH1 could compensate for the deadenylation defect caused by *caf1Δ*. In analyzing the steady-state *MFA2pG* levels, over-expression of *DHH1*, however, had no effect on the deadenylation defects observed with the *caf1-1*, *-6* and *caf1Δ* alleles (data not shown). In each of these strains, the *MFA2pG* mRNA did

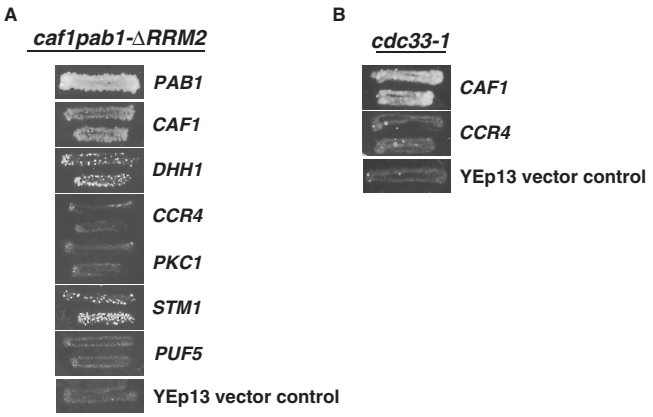

Figure 7. High-copy suppressors of *caf1Δ PAB1-ΔRRM2* lethality. (**A**) Over-expression of *DHH1* and *STM1* suppress the synthetic lethality of the *caf1Δ PAB1-ΔRRM2* double mutant. Strain ASY319-c1-lN/YC360 (*PAB1-URA3*)/YC506 (*PAB1-ΔRRM2-TRP1*) was transformed with YEp13 plasmids carrying MPT0 (*CAF1*), MPT1 (*DHH1*), MPT2 (*CCR4*), MPT3 (*PKC1*), MPT4 (*STM1*), MPT5 (*PUF5*) (29) and *PAB1*, respectively. Transformants were selected on minimal medium lacking leucine and tryptophan and replica plated to medium containing FOA to lose the YC360 plasmid. For the *DHH1* and *MPT4* complementation of *caf1Δ PAB1-ΔRRM2* lethality, the papillation of colonies that is observed are not revertants as they represent cells that begin growth at the same time that cells begin to grow in the control *PAB1* or *CAF1* situations. Similar papillations are typically observed for growth on 5′-FOA plates during the selection for loss of YC360 plasmids in many other experiments. (**B**) Over-expression of *CAF1* can suppress the caffeine sensitivity associated with the *cdc33-1* allele. Strain 1881/YC360 was transformed with MPT0, MPT2 or YEp13. The YD plates contained 8 mM caffeine.

not deadenylate completely and had longer poly(A) tail lengths than the wild-type regardless of whether *DHH1* was over-expressed or not. We additionally tested whether DHH1 association with the CAF1 variants was altered, as it has been shown that NOT1 and CAF1 can associate with DHH1 (33,34). DHH1 interaction with the CCR4-NOT complex for each of the CAF1 variants, however, was unaffected (Supplementary Figure 3), in agreement with previous data that showed that a *caf1* deletion had little effect on DHH1 association with NOT1 (33).

As DHH1 is involved in translation processes (34,35) and STM1 can interact with the ribosome and eIF4E and is important for protein synthesis (39–43), we determined whether over-expression of *CAF1* or *CCR4* could in turn complement a defect in translation factor eIF4E (*cdc33-1* allele). As shown in Figure 7B, over-expression of *CAF1* but not that of *CCR4* could complement the caffeine sensitivity displayed in a strain carrying the *cdc33-1* allele. As *cdc33-1* is specifically defective in binding the 5′ mRNA cap (44), these results provide further support for a functional interaction of CAF1 with translational factors distinct from the role of CCR4 in deadenylation. However, as over-expression of *CAF1* was found neither to rescue the *cdc33-1* defect in *in vivo* protein translation nor did it affect *in vivo* protein translation in a wild-type background (data not shown), over-expression of *CAF1* does not probably restore eIF4E function completely.

Because of the genetic interaction between *CAF1* and that of *cdc33-1*, we also assessed whether a *caf1Δ* could affect translation directly. Two aspects were analyzed. First, we conducted polysome profiles of mRNA isolated from wild-type and *caf1Δ* strains. No differences between the polysome profiles were observed (data not shown). Second, we assayed if a *caf1Δ* affected the rate of *in vivo* protein translation by quantitating the rate of incorporation of [^{35}S]-methionine into newly synthesized protein. A *caf1Δ* was found to reduce the rate of *in vivo* translation to 35% of wild type. In contrast, a *ccr4Δ* reduced *in vivo* translation only to 55% of wild type. SEMs for these series of experiments were <5% of the values. Similarly, in a *cdc33-1* background, a *caf1Δ* deletion reduced the rate of *in vivo* protein synthesis from 35% (*cdc33-1*) to that of 13% (*cdc33-1 caf1Δ*); the rate of protein synthesis was reduced to 24% by combining *cdc33-1* with *ccr4Δ*. These results indicate that a *caf1Δ* was displaying an additional effect on protein translation than observed through its possible effects on CCR4.

If CAF1 were to functionally interact with PAB1 and/or the translation process, it might be expected that defects in PAB1 could, in turn, when combined with *caf1Δ*, specifically reduce deadenylation. We subsequently analyzed whether other less severe defects in the RRM2 domain of PAB1 in conjunction with a *caf1* deletion affected the deadenylation process. Two PAB1 variants are known to affect different PAB1 translational functions (38). PAB1-184 and PAB1-134 carry three amino acids substitutions each: PAB1-184 affects eIF4G binding *in vitro* and PAB1-134 has an undefined *in vitro* translation defect involving 5′-cap-dependent translation (38). We first analyzed the effect of these variants on the steady-state distribution of poly(A) tail lengths for *GAL1*-L mRNA in conjunction with a *caf1* deletion. *caf1Δ PAB1-134* resulted in significantly longer steady-state *GAL1*-L poly(A) tail lengths as compared to *caf1Δ* alone, indicative of a slowed deadenylation rate (Figure 8A, right panel; data not shown), whereas *PAB1-184* had no effect on poly(A) tail lengths in conjunction with *caf1Δ*. This result suggests that both CAF1 and the PAB1-134 mutated residues are required for complete deadenylation. In contrast, *PAB1-134* in combination with *ccr4Δ* did not affect the steady-state distribution of *GAL1*-L poly(A) tail length as compared to *ccr4Δ* alone (Figure 8A; middle panel) nor did it affect the *GAL1*-L poly(A) tail lengths with wild-type PAB1 (Figure 8A, left panel). These latter results demonstrate that PAB1-134 is not affecting PAN2/3 deadenylase activity, which is the only deadenylase activity present in a strain lacking CCR4 (6).

Analysis of the actual deadenylation rate for *GAL1*-L showed that a *caf1Δ PAB1-134* background caused a severe slowing of the rate of deadenylation (0.7 A's/min compared to 4.0 A's/min for wild-type *PAB1* and 2.2 A's/min for *caf1Δ*) (Figure 8B). This slowing of the rate of deadenylation by *caf1Δ PAB1-134* was as severe as that observed in a *ccr4* deletion (Figure 8C; 1.1 A's/min). These observations suggest that defects in translation caused by PAB1-134 can cause corresponding defects in deadenylation and that proper translation in conjunction with

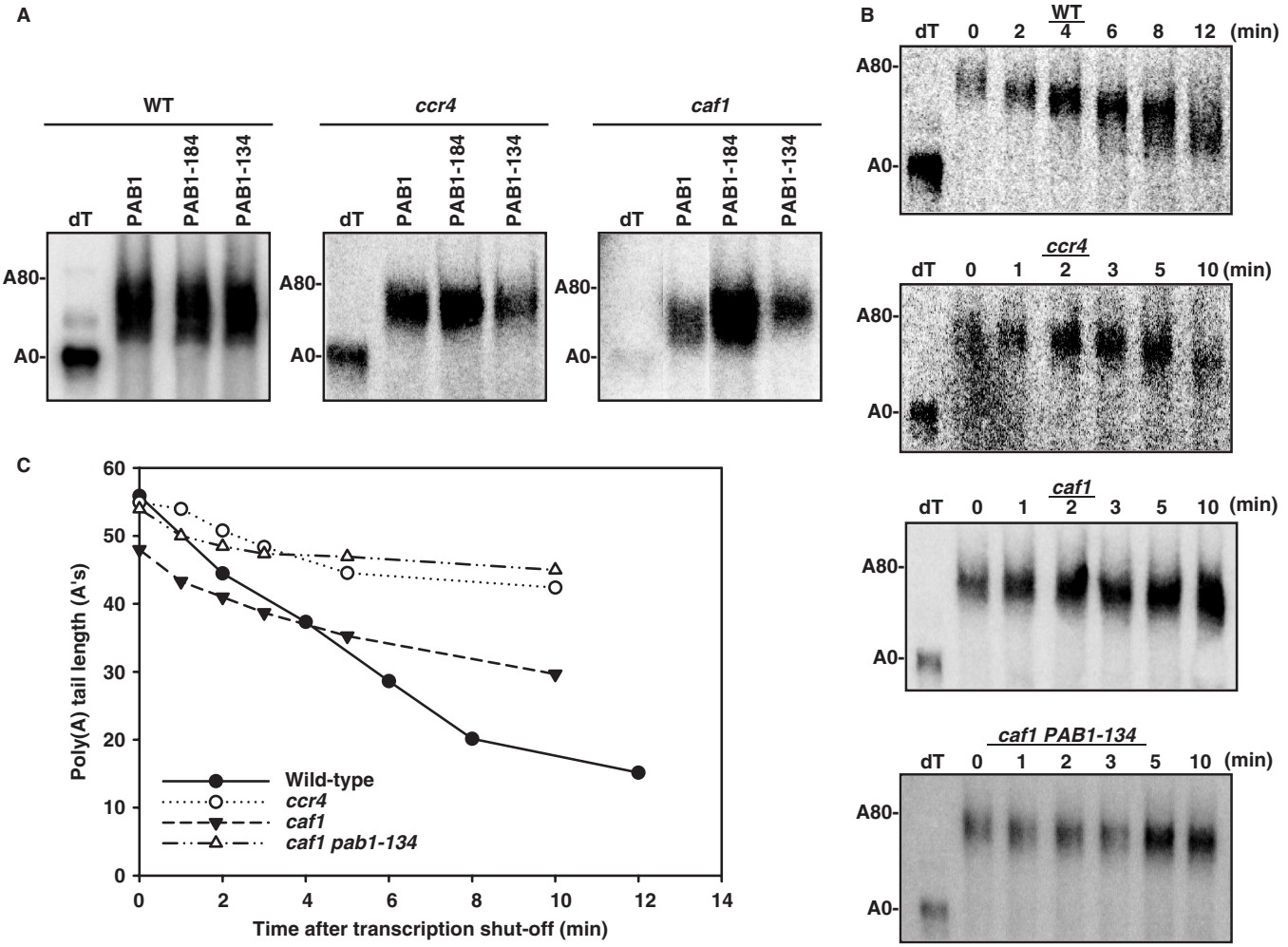

Figure 8. PAB1-134 blocks deadenylation in a *caf1Δ* background. (**A**) Steady-state mRNA analysis of *GAL1* was conducted as described in the Materials and Methods section. wt- AS319; *ccr4Δ*- AS319-1a-uN; *caf1Δ*-AS319-c1-lN. (**B**) Pulse-chase analysis of *GAL1*-L mRNA deadenylation was conducted as described in Figure 4. PAB1-134 refers to AS319/YC545 and PAB1-184 refers to AS319/YC538. YC545 expresses the PAB1 protein with residues 134HPD137 replaced with DKS and YC538 has residues 184DAL187 of PAB1 replaced with EKM (38). PAB1-134 and PAB1-184 were expressed in yeast to levels comparable to that of wild-type PAB1 (Supplementary Figure 4). (**C**) The graphical representation of the deadenylation rate analyses from (B).

CAF1 is required for complete deadenylation by CCR4 (see Discussion). Because the PAB1-134 protein had only been assessed for effects on *in vitro* translation (38), it remains possible that PAB1-134 does not affect *in vivo* translation. We consequently determined if PAB1-134 was defective for *in vivo* translation by quantitating the rate of incorporation of [^{35}S]-methionine into newly synthesized protein. PAB1-134 did not affect the rate of *in vivo* translation as compared to PAB1 wild type (data not shown). However, when we combined *PAB1-134* with a defect in eIF3 (*prt1-63* allele) that has previously been shown to reduce the rate of *in vivo* translation (24), we found that *PAB1-134 prt1-63* reduced the rate of *in vivo* translation significantly compared to *prt1-63* alone: *prt1-63 PAB1-134* ($31 \pm 5.0\%$), *prt1-63* ($45 \pm 3.0\%$), and wild type (100%). In contrast, *PAB1-184* did not affect *in vivo* translation alone or in conjunction with *prt1-63* ($48 \pm 7.5\%$). These results indicate that the PAB1-134 protein does display defects for *in vivo* translation.

DISCUSSION

It has been shown that the CAF1 C-terminal domain purified from *E. coli* exhibits an exonuclease activity with a poly(A) preference (19,23). Our previous mutation studies of CAF1 established, however, that its RNase function is not required for the *in vivo* deadenylation process (16). This discrepancy prompted us to identify the functional domains that are critical for CAF1 to perform its role in mRNA turnover. By targeting only those sequences absolutely conserved amongst all CAF1 orthologs but not present in other members of the DEDDh family of nucleases, we sought to identify CAF1-specific functions. This methodology led us to define several separable functional regions in the CAF1 protein.

Immunoprecipitation analyses with *CAF1* mutants used in this study showed that three amino acids (213FRS215) deleted in *caf1-2* are most required for the CAF1

interaction with CCR4. As mammalian CAF1 can also bind yeast CCR4, it would be expected that the CAF1 residues involved in this contact have been retained evolutionarily. Residues 213–215 are found in a loop region whose structure was not fixed enough to be determined in the X-ray analysis of CAF1 (Figure 1A) (19). Other residues of CAF1 might also be involved in contacting CCR4 as the caf1-1, -3, -5 and -6 proteins also displayed weakened binding to CCR4. The caf1-2 protein displayed a weak caffeine-sensitive phenotype and intermediate effects on deadenylation *in vivo* as compared to a *caf1* deletion or to mutations in other regions of the CAF1 protein that were capable of binding CCR4 to a much greater extent. It appears, therefore, that CAF1 binding to CCR4 is not the only function of CAF1 for deadenylation. This conclusion extends the results from our previous analysis wherein mutations in CCR4 that significantly reduced, albeit did not eliminate, CCR4 binding to CAF1 appeared phenotypically wild type (30).

In contrast to *caf1-2*, the most important regions for CAF1 function *in vivo* were identified by the *caf1-1*, *-3* and *-6* alleles. These three *caf1* mutant alleles displayed severe defects in poly(A) shortening like that of a *caf1* deletion and were as caffeine sensitive as the *caf1* deletion. Three observations suggest that *caf1-1* and *caf1-3* alleles are equivalent physically and functionally. First, the X-ray crystal structure showed that *caf1-1* and *caf1-3* alleles are located in the same region where two parallel β strands (β1 and β4) are aligned side by side (Figure 1A) (19). The exact locations of caf1-1 and caf1-3 in these β strands indicate that each triplet of residues do not actually H-bond with each other, but lie contiguous along the β sheet structure (19). Each defect would be expected to partially disrupt this region of the β sheet structure. Second, yeast cells carrying either of the two alleles grew more slowly than did a *caf1* deletion. Third, both alleles showed similar *GAL1* deadenylation rates and defects in *MFA2pG* endpoints. These observations indicate that the *caf1-1* and *caf1-3* alleles define a novel functional region of yeast CAF1 required for its cellular activity. The *caf1-6* allele, deleting residues 340DFE342, defines a third functional region of CAF1. Phenotypes associated with *caf1-6* are nearly identical to those observed for *caf1-1* and *-3*, although the location of the *caf1-6* mutation is on the opposite site of the CAF1 protein as that of *caf1-1* and *-3*. It is unlikely, however, that the putative contacts made by the caf1-6 region (α8) are to the same factors as presumed to contact the β1 and β4 sheets. At least, both regions and their putative contacts are central to CAF1 *in vivo* function.

In regards to the location of the six mutations in the structure of CAF1, the following observations can be made. First, none of the mutations are either in the presumed catalytic area (α4 and α5 and the loop between the β2 and β3 strands) or in the negatively charged cavity of CAF1 that coincides with the active site found in the structurally and evolutionarily related ε subunit of DNA polymerase III (polIII) or DNA polymerase I (polI) (19). Second, the β1 strand of CAF1 (the site of the *caf1-1* alteration) is not found in polIII, although it is present in polI. The sequence features of β4 that were mutated in *caf1-3* are alternating non-polar/polar/non-polar residues, a pattern retained by both polIII and polI, albeit with distinctly different residues for the polar residues and different sizes for the non-polar amino acids. Third, the whole protein region corresponding to α8, the turn region after α7, and the loop between β2 and α3, the sites of the *caf1-6*, *-5* and *-2* mutations, respectively, is not present in either polIII or polI. These three sites are all close to one another and are located on the exterior of the protein. The evolutionary conservation of this region across the CAF1 protein family argues for unique contacts made by it, including but not limited to binding CCR4.

In that we also observed that none of our *CAF1* alleles severely affected *in vitro* CCR4 deadenylation activity regardless of whether the alleles blocked CCR4 binding to CAF1 (*caf1-2*) or not, we conclude that CAF1 does not directly regulate CCR4 activity *in vitro*. This is in agreement with our previous observations (7,30). Also, as mentioned above each of the *CAF1* alleles interacted equivalently well with NOT1, further suggesting that the identified roles for CAF1 *in vivo* are not solely defined through this interaction either. Yet, because binding to NOT1 was reduced by each of the defective CAF1 proteins, it remains possible that disruptions in the CAF1-NOT1 interaction are responsible for at least part of the reductions in deadenylation that were observed. Moreover, in that DHH1 is known to contact the CCR4-NOT complex through the N-terminal part of NOT1 (33), the genetic interactions observed between DHH1 and CAF1 could be mediated in part by NOT1.

Because the *caf1-1*, *-3* and *-6* alleles resulted in more significant defects in deadenylation than did the *caf1-2* allele, CAF1 appears to function to control the deadenylation process through non-CCR4 contacts in addition to its contact to CCR4. As mentioned above, disrupting the NOT1 contact does not seem to be solely responsible for this phenotype and we showed that all of the CAF1 variants interacted equivalently with DHH1. The genetic analyses demonstrating *caf1Δ* but not *ccr4Δ* lethality with the decapping/translation regulator *dhh1Δ* and with *PAB1-ΔRRM2/ΔRRM1* is consistent with CAF1 exerting effects separate from CCR4. However, neither of these lethalities is probably due solely to deadenylation defects that are more severe than those observed in a *ccr4Δ* background in that the total lack of deadenylation in yeast is not lethal (6; data not shown). As it has been observed that a *caf1* deletion does not result in more severe decapping defects than does *ccr4Δ* (5,6; data not shown), it is also unlikely that CAF1 is exerting these other effects through decapping (6). Rather, it appears that CAF1 in conjunction with DHH1 and with PAB1 is required for some other essential process.

In terms of the role of CAF1 in deadenylation, CAF1 appears to play at least two roles. First, through its contact to CCR4 it aids CCR4 association to the CCR4-NOT complex that is important for CCR4 deadenylation. Second, it may affect some aspect of translation that in turn interferes with deadenylation and/or act on deadenylation in conjunction with factors such as PAB1 and DHH1 that play roles in translation. Several observations support this inference. Deleting those

domains of PAB1 that are known to affect *in vivo* and *in vitro* translation were lethal with deleting *CAF1*. In addition to the observed lethalities described above, we found that over-expression of translational regulator *DHH1* and ribosome-associated protein *STM1* can specifically suppress the *caf1Δ PAB1-ΔRRM2* lethality. Other suppressors of *caf1Δ* not as directly involved in translation, such as *CCR4*, *PKC1* and *PUF5*, did not display this phenotype. We also showed that over-expression of *CAF1* but not that of *CCR4* could suppress phenotypes associated with a defect in translation factor eIF4E. In addition, a *caf1Δ* slowed *in vivo* protein synthesis, although how it does this is not clear. Taken together, these data point to a role for CAF1 in functionally interacting with translationally important proteins.

A possible role for translation or factors involved in translation in being required for deadenylation was supported by the observation that the PAB1-134 variant slowed the rate of deadenylation when combined with a *caf1* deletion. PAB1-134 did not affect deadenylation by itself and had no effect on deadenylaton when combined with a *ccr4* deletion. The PAB1-134 protein is known to be defective for *in vitro* translation (38), and we showed that it reduced *in vivo* translation when combined with defects in translation initiation factors. Previous studies have indicated that defects in translation initiation factors accelerated the CCR4 deadenylation process (24). In these cases, interference with translation initiation would appear to predispose the mRNP for deadenylation and should not necessarily inhibit it. In contrast, the *PAB1-134 caf1Δ* effect on deadenylation implies that both PAB1 and CAF1 are required for deadenylation. As PAB1 has been suggested to both inhibit and be required for deadenylation (5,45,46), additional studies are necessary to clarify how other factors of the mRNP, such as PAB1, actually affect CCR4 deadenylation. Their analysis may shed light on the means by which CAF1 affects the mRNA degradation process.

SUPPLEMENTARY DATA

Supplementary Data are available at NAR online.

ACKNOWLEDGEMENTS

We would like to thank R. Parker, D. Mangus and D. Belostotsky for plasmids used in this study. This research was supported by NIH grants GM41215 and GM78078, and by Hatch award H291. This is Scientific Contribution Number 2277 from the New Hampshire Agricultural Experiment Station. Funding to pay the Open Access publication charges for this article was provided by the New Hampshire Agricultural Experiment Station.

Conflict of interest statement. None declared.

REFERENCES

1. Parker,R. and Song,H. (2004) The enzymes and control of eukaryotic mRNA turnover. *Nat. Struct. Mol. Biol.*, **11**, 121–127.
2. Beelman,C.A. and Parker,R. (1995) Degradation of mRNA in eukaryotes. *Cell*, **81**, 179–183.
3. Wilusz,C.J., Wormington,M. and Peltz,S.W. (2001) The cap-to-tail guide to mRNA turnover. *Nat. Rev. Mol. Cell Biol.*, **2**, 237–246.
4. Cao,D. and Parker,R. (2001) Computational modeling of eukaryotic mRNA turnover. *RNA*, **7**, 1192–1212.
5. Tucker,M., Staples,R.R., Valencia-Sanchez,M.A., Muhlrad,D. and Parker,R. (2002) Ccr4p is the catalytic sub-unit of a Ccr4/Pop2p/Notp mRNA deadenylase complex in *Saccharomyces cerevisiae*. *EMBO J.*, **21**, 1427–1436.
6. Tucker,M., Valencia-Sanchez,M.A., Staples,R.R., Chen,J., Denis,C.L. and Parker,R. (2001) The transcription factor associated Ccr4 and Caf1 proteins are components of the major cytoplasmic mRNA deadenylase in *Saccharomyces cerevisiae*. *Cell*, **104**, 377–406.
7. Chen,J., Chiang,Y.-C. and Denis,C.L. (2002) CCR4, a 3′-5′ poly(A) RNA and ssDNA exonuclease, is the catalytic component of the cytoplasmic deadenylase. *EMBO J.*, **21**, 1414–1426.
8. Liu,H.-Y., Badarinarayana,V., Audino,D.C., Rappsilber,J., Mann,M. and Denis,C.L. (1998) The NOT proteins are part of the CCR4 transcriptional complex and affect gene expression both positively and negatively. *EMBO J.*, **17**, 1096–1106.
9. Bai,Y., Salvadore,C., Chiang,Y.-C., Collart,M., Liu,H.-Y. and Denis,C.L. (1999) The CCR4 and CAF1 proteins of the CCR4-NOT complex are physically and functionally separate from NOT2, NOT4, and NOT5. *Mol. Cell. Biol.*, **19**, 6642–6651.
10. Chen,J., Rappsilber,J., Chiang,Y.-C., Russell,P., Mann,M. and Denis,C.L. (2001) Purification and characterization of the 1.0 MDa CCR4-NOT complex identifies two novel components of the complex. *J. Mol. Biol.*, **314**, 683–694.
11. Denis,C.L. and Chen,J. (2003) The CCR4-NOT complex plays diverse roles in mRNA metabolism. *Nucl. Acids Res. Mol. Biol.*, **73**, 221–250.
12. Dlakic,M. (2000) Functionally unrelated signaling proteins contain a fold similar to Mg^{2+}-dependent endonucleases. *Trends Biochem. Sci.*, **25**, 272–273.
13. Dupressoir,A., Barbot,W., Loireau,M.P. and Hedmann,T. (1999) Characterization of a mammalian gene related to the yeast CCR4 general transcription factor and revealed by transposon insertion. *J. Biol. Chem.*, **274**, 31068–31075.
14. Temme,C., Zaessinger,S., Meyer,S., Simonelig,M. and Wahle,E. (2004) A complex containing the CCR4 and CAF1 proteins is involved in mRNA deadenylation in *Drosophila*. *EMBO J.*, **23**, 2862–2871.
15. Draper,M.P., Salvadore,C. and Denis,C.L. (1995) Identification of a mouse protein whose homolog in *Saccharomyces cerevisiae* is a component of the CCR4 transcriptional regulatory complex. *Mol. Cell. Biol.*, **15**, 487–495.
16. Viswanathan,P., Ohn,T., Chiang,Y.-C., Chen,J. and Denis,C.L. (2004) Mouse CAF1 can function as a processive deadenylase/3′-5′-exonuclease *in vitro* but in yeast the deadenylase function of CAF1 is not required for mRNA poly(A) removal. *J. Biol. Chem.*, **279**, 23988–23995.
17. Moser,M.J., Holley,W.R., Chatterjee,A. and Mian,I.S. (1997) The proofreading domain of *Escherichia coli* DNA polymerse I and other DNA and/or RNA exonuclease domain. *Nucleic Acids Res.*, **25**, 5110–5118.
18. Zuo,Y. and Deutscher,M.P. (2001) Exoribonuclease superfamilies: structural analysis and phylogenetic distribution. *Nucleic Acids Res.*, **29**, 1017–1026.
19. Thore,S., Mauxion,F., Séraphin,B. and Suck,D. (2003) X-ray structure and activity of the yeast Pop2 protein: a nuclease subunit of the mRNA deadenylase complex. *EMBO Rep.*, **4**, 1150–1155.
20. Daugeron,M.-C., Mauxion,F. and Séraphin,B. (2001) The yeast *POP2* gene encodes a nuclease involved in mRNA deadenylation. *Nucleic Acids Res.*, **29**, 2448–2455.
21. Goldstrohm,A.C., Hook,B.A., Seay,D.J. and Wickens,M. (2006) PUF proteins bind Pop2p to regulate messenger RNAs. *Nat. Struct. Mol. Biol.*, **13**, 533–539.
22. Cook,W.J., Chase,D., Audino,D.C. and Denis,C.L. (1994) Dissection of the ADR1 protein reveals multiple, functionally

redundant activation domains interspersed with inhibitory regions: evidence for a repressor binding to the ADR1^c region. *Mol. Cell. Biol.*, **14**, 629–640.
23. Viswanathan,P., Chen,J., Chiang,Y.-C. and Denis,C.L. (2003) Identification of multiple RNA features that influence CCR4 deadenylation activity. *J. Biol. Chem.*, **278**, 14949–14955.
24. Schwartz,D.C. and Parker,R. (1999) Mutations in translation initiation factors lead to increased rates of deadenylation and decapping of mRNAs in *Saccharomyces cereviseae*. *Mol. Cell. Biol.*, **19**, 5247–5256.
25. Cook,W.J. and Denis,C.L. (1993) Identification of three genes required for the glucose-dependent transcription of the yeast transcriptional activator ADR1. *Curr. Genet.*, **23**, 192–200.
26. Muhlrad,D. and Parker,R. (1992) Mutations affecting stability and deadenylation of the yeast *MFA2* transcript. *Genes Dev.*, **6**, 2100–2111.
27. Moriya,H., Shimizu-Yoshida,Y., Omori,A., Iwashita,S., Katoh,M. and Sakai,A. (2001) Yak1p, a DYRK family kinase, translocates to the nucleus and phosphorylates yeast Pop2p in response to a glucose signal. *Genes Dev.*, **15**, 1217–1228.
28. Sakai,A., Chibazakura,T., Shimizu,Y. and Hishinuma,F. (1992) Molecular analysis of *POP2* gene, a gene required for glucose-derepression of gene expression in *Saccharomyces cerevisiae*. *Nucleic Acids Res.*, **20**, 6227–6233.
29. Hata,H., Mitsui,H., Liu,H.-Y., Bai,Y., Denis,C.L., Shimizu,Y. and Sakai,A. (1998) Dhh1p, a putative RNA helicase, associates with the general transcription factors Pop2p and Ccr4p from *Saccharomyces cerevisiae*. *Genetics*, **148**, 571–579.
30. Clark,L.C., Viswanathan,P., Quigley,G., Chiang,Y.-C., McMahon,J.S., Yao,G., Chen,J., Nelsbach,A. and Denis,C.L. (2004) Systematic mutagenesis of the leucin-rich repeat (LRR) domain of CCR4 reveals specific sites for binding to CAF1 and a separate critical role for the LRR in CCR4 deadenylase activity. *J. Biol. Chem.*, **279**, 13616–13623.
31. Cui,Y. and Denis,C.L. (2003) In vivo evidence that defects in the transcriptional elongation factors RPB2, TFIIS, and SPT5 enhance upstream poly(A) site utilization. *Mol. Cell. Biol.*, **23**, 7887–7910.
32. Miyajima,A., Nakayama,N., Miyajima,I., Arai,N., Okayama,H. and Arai,K. (1984) Analysis of full-length cDNA clones carrying GAL1 of *Saccharomyces cerevisiae*: a model system for cDNA expression. *Nucleic Acids Res.*, **12**, 6397–6414.
33. Maillet,L. and Collart,M.A. (2002) Interaction between Not1p, a component of the Ccr4 complex, a global regulator of transcription, and Dhh1p, a putative RNA helicase. *J. Biol. Chem.*, **277**, 2835–2842.
34. Coller,J.M., Tucker,M., Sheth,U., Valencia-Sanchez,M.A. and Parker,R. (2001) The DEAD box helicase, Dhh1p, functions in mRNA decapping and interacts with both the decapping and deadenylase complexes. *RNA*, **7**, 1717–1727.
35. Coller,J.M. and Parker,R. (2005) General translational repression by activators of mRNA decapping. *Cell*, **122**, 875–886.
36. Deardorff,J.A. and Sachs,A.B. (1997) Differential effects of aromatic and charged residue substitutions in the RNA binding domains of the yeast poly(A)-binding protein. *J. Mol. Biol.*, **269**, 67–81.
37. Kessler,S.H. and Sachs,A.B. (1998) RNA recognition motif 2 of yeast Pab1p is required for its functional interaction with eukaryotic translation initiation factor 4G. *Mol. Cell. Biol.*, **18**, 51–57.
38. Otero,L.J., Ashe,M.P. and Sachs,A.B. (1999) The yeast poly(A)-binding protein Pab1p stimulates in vitro poly(A)-dependent and cap-dependent translation by distinct mechanisms. *EMBO J.*, **18**, 3153–3163.
39. Van Dyke,N., Baby,J. and Van Dyke,M.W. (2006) Stm1p, a ribosome-associated protein, is important for protein synthesis in *Saccharomyces cerevisiae* under nutritional stress conditions. *J. Mol. Biol.*, **358**, 1023–1031.
40. Van Dyke,M.W., Nelson,L.D., Weilbaecher,R.G. and Mehta,D.V. (2004) Stm1p, a G_4 quadruplex and purine motif triplex nucleic acid-binding protein, interacts with ribosomes and subtelomeric Y' DNA in *Saccharomyces cerevisiae*. *J. Biol. Chem.*, **279**, 24323–24333.
41. Gavin,A.C., Bosche,M., Krause,R., Grandi,P., Marzioch,M., Bauer,A., Schultz,J., Rick,J.M., Michon,A.-M. *et al.* (2002) Functional organization of the yeast proteome by systemic analysis of protein complexes. *Nature*, **415**, 141–147.
42. Inada,T., Winstall,E., Tarun,S.Z.Jr, Yates,J.R.III, Schieltz,D. and Sachs,A.B. (2002) One-step affinity purification of the yeast ribosome and its associated proteins and mRNAs. *RNA*, **8**, 948–956.
43. Takaku,H., Mutoh,E., Horiuchi,H., Ohta,A. and Takagi,M. (2001) Ray38p, a homolog of a purine motif triple-helical DNA-binding protein, Stm1p, is a ribosome-associated protein and dissociated from ribosomes prior to the induction of cycloheximide resistance in Candida maltosa. *Biochem. Biophys. Res. Commun.*, **284**, 194–202.
44. Altmann,M. and Trachsel,H. (1989) Altered mRNA cap recognition activity of initiation factor 4E in the yeast cell cycle division mutant cdc33. *Nucleic Acids Res.*, **17**, 5923–5931.
45. Caponigro,G. and Parker,R. (1995) Multiple functions for the poly(A)-binding protein in mRNA decapping and deadenylation in yeast. *Genes Dev.*, **9**, 2421–2432.
46. Morrissey,J.P., Deardorff,J.A., Hebron,C. and Sachs,A.B. (1999) Decapping of stabilized, polyadenylated mRNA in yeast pab1 mutants. *Yeast*, **15**, 687–702.